Quantification of t-tubule area and protein distribution in rat cardiac ventricular myocytes.

Michal Pásek, Fabien Brette, Adam Nelson, C. Pearce, A. Qaiser, Georges Christé, Clive H. Orchard

Quantification of t-tubule area and protein distribution in rat cardiac ventricular myocytes

M. Pasek*, F. Brette[#] A. Nelson[§], C. Pearce[¶], A. Qaiser[¶], G. Christe[†], and C.H. Orchard[¶]

* Institute of Thermomechanics, Czech Academy of Science - branch Brno, and Department of Physiology, Faculty of Medicine, Masaryk University, Brno, Czech Republic

[#] Faculty of Life Sciences, University of Manchester, Manchester, M13 9NT, United Kingdom

[§] Centre for Self Organising Molecular Systems, University of Leeds, Leeds LS2 9JT, United Kingdom

[¶] Department of Physiology, University of Bristol, Bristol, BS8 1TD, United Kingdom

[†] INSERM, Lyon, France

Correspondence to Clive Orchard at the above address[¶]
e-mail: clive.orchard@bristol.ac.uk
tel: +44-(0)117-331-7289

Running head: t-tubule quantification

Abstract

The transverse (t-) tubules of cardiac ventricular myocytes are invaginations of the surface membrane that form a complex network within the cell. Many of the key proteins involved in excitation-contraction coupling appear to be located predominantly at the t-tubule membrane. Despite their importance, the fraction of cell membrane within the t-tubules remains unclear: measurement of cell capacitance following detubulation suggests ~32%, whereas optical measurements suggest up to ~65%. We have therefore investigated the factors that may account for this discrepancy. Calculation of the combinations of t-tubule radius, length and density that produce t-tubular membrane fractions of 32% or 56% suggest that the true fraction is at the upper end of this range. Assessment of detubulation using confocal and electron microscopy suggests that incomplete detubulation can account for some, but not all of the difference. High cholesterol, and a consequent decrease in specific capacitance, in the t-tubule membrane, may also cause the t-tubule fraction calculated from the loss of capacitance following detubulation to be underestimated. Correcting for both of these factors results in an estimate that is still lower than that obtained from optical measurements suggesting either that optical methods overestimate the fraction of membrane in the t-tubules, or that other, unknown, factors, reduce the apparent fraction obtained by detubulation. A biophysically realistic computer model of a rat ventricular myocyte, incorporating a t-tubule network, is used to assess the effect of the altered estimates of t-tubular membrane fraction on the calculated distribution of ion flux pathways.

Key words: cardiac myocyte, t-tubule, electrophysiology, excitation-contraction coupling, capacitance, cholesterol.

Introduction

During the cardiac action potential, Ca influx via L-type Ca channels activates ryanodine receptors in adjacent sarcoplasmic reticulum (SR) membrane, causing Ca release from the SR (Bers, 2002). In ventricular myocytes Ca influx, and hence Ca release, occurs predominantly at invaginations of the surface membrane called transverse (t-) tubules (Brette & Orchard, 2003). This causes spatial and temporal synchronization of Ca release, and hence synchronized contraction of the cell (Wier & Balke, 1999).

Recent work using ventricular myocytes has shown that uncoupling the t-tubules physically and functionally from the surface membrane (detubulation) results in loss of ~32% of cell capacitance (a function of membrane area), but ~87% of L-type Ca current (I_{Ca}), suggesting a high density of I_{Ca} in the t-tubules (Kawai $et\ al.$, 1999). However optical measurements suggest that the surface area of the t-tubules is 0.44 μm^2 per μm^3 cell volume (Soeller & Cannell, 1999); normalized to the estimated total surface area/cell volume of a myocyte 100 μm long and 20 μm in diameter (0.68 $\mu m^2/\mu m^3$) this gives a t-tubular membrane fraction of 65% (Soeller & Cannell, 1999). This agrees with the lower capacitance (pF)/ cell volume (pl) ratio determined by Satoh $et\ al.$ (1996; 6.76 pF/pl in 3 month old rats, compared to 8.88 pF/pl in 6 month old rats): assuming a membrane capacitance of 1 $\mu F/cm^2$ these values give surface area/volume ratios of 0.676 and 0.888 $\mu m^2/\mu m^3$, and hence t-tubular fractions of 65% and 50%, respectively. Thus optical measurements suggest that the t-tubule fraction is higher than that obtained by detubulation. The reasons for this discrepancy are unclear.

If the fractional area of the t-tubule membrane is greater than estimated by detubulation, the density of membrane currents in the t-tubules would be lower than previously calculated, although the absolute amounts and relative concentrations would remain the same. This would have important implications for cell function and for the mechanisms trafficking and localizing proteins at the t-tubules.

The present study used a combination of modeling and experimental approaches to investigate the fraction of the cell membrane within the t-tubules, and its effect on the calculated distributions of ion flux pathways.

3

Methods

Computational methods

The computer model of the rat ventricular myocyte used in the present study has been described previously (Pasek *et al.,* 2006). The model was implemented in MATLAB 6.5 (MathWorks, Inc.) and was based on Pandit's quantitative description (Pandit *et al.*, 2001), modified to include a t-tubule compartment. The numerical computation of the system of 59 non-linear differential equations was performed using the solver for stiff systems ODE-15s. The model equations were simultaneously solved using a time step adjusted to keep the estimated relative error of inner variables below a threshold value of 0.001. After every change in model equations or parameter values, the model was run for 20 minutes of equivalent cell lifetime to ensure that steady-state was reached. The values of all variables at this time were assigned as starting values before running model trials. The units in which the equations were solved were: *mV* for membrane voltage, *μA* for membrane currents, *mM* for ion concentrations, *ml* for volumes and *s* for time.

Cell isolation and t-tubule imaging

Myocytes were isolated from the ventricles of Wistar rat hearts by enzymatic dissociation, and detubulated using formamide, as described previously (Brette *et al.*, 2002). To image the t-tubules the cells were stained with di-8-ANEPPS, and 1 μm optical sections were imaged at 8 bit resolution using a Zeiss Pascal confocal microscope; confocal images of control and detubulated myocytes stained with di-8-ANEPPS have been published previously (Brette *et al.*, 2002). Offset and gain were adjusted to use the entire dynamic range of the microscope. The area within the cell membrane was outlined manually using Zeiss image analysis software, and the contrast and brightness were increased to produce a binary image in which pixels with an intensity greater than the median were set to the maximum value (255) and those below the median value were set to 0. The total outlined area, and the area occupied by pixels with an intensity of 255 were measured, and used to calculate the percentage of the cell interior occupied by membranes accessible to staining from the extracellular space, which was taken to represent t-tubule membrane. This technique of "thresholding" and pixel counting is similar to that described previously (Heinzel *et al.*, 2002).

Electron Microscopy

Myocytes were fixed in 5% glyceraldehyde and 0.2 mol/l sodium cacodylate buffer (pH 7.2). After centrifugation and washing the cells were embedded in fresh resin and left for 48 hours. Sections for cutting were chosen after staining with methylene blue and visualisation using light microscopy. Thin longitudinal sections were cut on a Diatome diamond knife and collected on copper slotted grids coated in Pioloform film. The grids were stained with uranylacetate (10 minutes) and lead citrate (10 minutes) and viewed in a Philips CM100 transmission electron microscope (TEM). Myocytes were photographed using Kodak 4489 film at a resolution of 4622 pixels x 3831 pixels, and at x6600 magnification so that each μm was equal to 16.5 mm on the printed image. Analysis of these images was performed without knowing whether control or detubulated myocytes were being analysed.

Measurement of specific capacitance of DOPC membranes

Monolayers of dioleoyl phosphatidylcholine (DOPC) and DOPC + cholesterol were prepared as described previously (Bizzotto & Nelson, 1998;Cohen-Atiya *et al.*, 2006;Nelson & Auffret, 1988;Whitehouse *et al.*, 2004) by spreading 13 μl of a DOPC + cholesterol mixture in pentane (HPLC grade, Fisher Scientific Chemicals Ltd) at the argon-electrolyte interface in an electrochemical cell. A 2.55 mmol/l working solution of DOPC was obtained by dilution of a 63.7 mmol/l stock solution (Avanti Lipids). The cholesterol was prepared as a stock solution of 10.3 mmol/l. Aliquots were taken from the cholesterol stock solution and added to the DOPC working solution to give a specified mole fraction of cholesterol in DOPC. A fresh mercury drop (area = 0.0088 cm^2) was coated with the DOPC and cholesterol mixed layer at the argon-electrolyte interface before each series of experiments. Although the DOPC and cholesterol were about four times excess of surface coverage at the argon-water interface, the coverage of the monolayer on the mercury surface subsequent to transfer was always neither less than, nor in excess of, full coverage. This is because the lipid coverage on the electrode is always controlled by the configuration of the carefully prepared electrode capillary and not by the coverage at the argon-electrolyte interface (Cohen-Atiya *et al.*, 2006).

The specific capacitance of DOPC monolayers and DOPC monolayers + cholesterol was measured as zero frequency capacitance using electrochemical techniques of impedance: measurements of impedance (Z) versus frequency (f) of the electrode systems using frequencies logarithmically distributed from 65000 to 0.1 Hz, *ac* amplitude (ΔE) 0.005 *V* at potential -0.4 V were carried out on the coated electrode systems. The impedance data were transformed to the complex capacitance

plane and the complex capacitance axes were expressed as Re $Y\,\omega^{-1}$ and Im $Y\,\omega^{-1}$ respectively, using the EXCEL (Microsoft) spreadsheet. For a series RC circuit, the Re $Y\,\omega^{-1}$ versus Im $Y\omega^{-1}$ plot gives a single semi-circle for the RC element, where the capacitor has no frequency dispersion. A monolayer of DOPC behaves as a simple capacitor in a RC circuit appearing as a single semi-circle in the complex capacitance plot. The incorporation of cholesterol into the DOPC monolayer at mole fractions of 0.3 and above gives rise to the occurrence of low frequency relaxations in the complex capacitance plot. The extrapolation of the RC semi-circle to the Im Y ω^{-1} axis at low frequency gives the zero frequency capacitance (C) of the RC circuit which is the specific capacitance of the monolayer. These methods applied to the specific capacitance of DOPC monolayers are described in detail (Whitehouse *et al.*, 2004).

Statistics

Data are presented as mean ± sem of n observations. Data were compared using paired or unpaired t-tests as appropriate, and significance taken as P<0.05.

Results

Which estimate of t-tubule membrane area is correct?

Membrane capacitance is a function of membrane area, and decreases by ~32% after detubulation (Brette *et al.*, 2002;Brette *et al.*, 2004a;Brette *et al.*, 2004b;Brette & Orchard, 2006b;Brette & Orchard, 2006a;Brette *et al.*, 2006b;Despa *et al.*, 2003;Kawai *et al.*, 1999;Komukai *et al.*, 2002;Yang *et al.*, 2002). This is similar to the fraction of cell membrane estimated to be in the t-tubules using electron microscopy (Page, 1978). However structural and sampling distortions can occur during preparation of tissue for electron microscopy, and measurements obtained by filling the t-tubules of a living cell with fluorescent dye (Soeller & Cannell, 1999) combined with measurements of surface/volume ratio (Satoh *et al.*, 1996) suggest that >50% of the cell membrane is within the t-tubules (Bers, 2001). We have used a simple model to explore this discrepancy: we determined the combinations of t-tubule radius, length and density that produce either 32% (the value obtained by detubulation) or 56% (a value computed from optical measurements and the average surface/volume ratio of 0.782 $\mu m^2/\mu m^3$ from Satoh *et al.* 1996; above). We thus determined whether using 32% or 56% gave combinations of these variables that were close to those observed experimentally. To do this, we used the derived relationship:

$$F_t /(1-F_t) = 2\pi r_t l_t dens_t$$

where F_t is the fraction of cell membrane within the t-tubules, r_t is t-tubule radius, l_t is t-tubule length and $dens_t$ is t-tubule density, expressed as the number of t-tubule openings per unit area of surface membrane. The planes in figure 1 show solutions to this equation over the range of t-tubule radii and densities reported experimentally. These data show that the plane produced using a fractional area of 56 % contains tubular lengths in the range reported for the average length of tubular inter-branch segments (average 6.9 µm; Soeller & Cannell, 1999), whereas a fractional area of 32% produces lengths <4 µm, which is less than half the diameter of a cardiac myocyte and shorter than observed experimentally. These data suggest that a fractional value of 56% may be closer to the actual value than 32%. This raises the question of why the estimated fraction of cell membrane within the t-tubules is different using the two techniques. One possibility is that the optical dye-filling technique overestimates the fraction of membrane in the t-tubules, although the data presented above makes this less likely. Alternatively detubulation may under-estimate the fraction of cell membrane within the t-tubules, either because some t-tubules remain coupled to the

surface membrane or because the specific capacitance of the t-tubule membrane is lower than that of the surface membrane, so that a greater fraction of membrane is lost than capacitance. These possibilities are considered further below.

Could incomplete detubulation contribute to the discrepancy?

To address the first of these possibilities, the extent of detubulation was estimated from confocal images of intact and detubulated rat ventricular myocytes stained with the lipophilic dye di-8-ANEPPS and imaged as described in Methods. These cells were from cell isolations used for previously published work, in which detubulation was used to determine the distribution of ion flux pathways between the t-tubule and surface membranes. t-tubule staining was determined by "thresholding" as described in Methods. In 12 control cells, $15.28 \pm 2.22\%$ of the cell interior showed such staining; in 8 detubulated cells, the value was $1.17 \pm 0.29\%$, suggesting that following detubulation 7.7% of the t-tubule network remained accessible to the extracellular space. This will contribute to, but is insufficient to account for, the discrepancy between the optical and electrophysiological measurements of t-tubule membrane fraction.

To investigate whether ultrastructural distortion of the t-tubules following detubulation might alter the apparent membrane area, electron microscopy was used to image intact and formamide-treated (detubulated) myocytes. Representative images are shown in figure 2 (left). Attempts to use prior labelling with lanthanum, as described previously for skeletal muscle (e.g. Voigt and Dauber 2004), to identify and image the t-tubules, were unsuccessful, and would in any case not penetrate t-tubules that are inaccessible from the extracellular space. Thus spaces in the image were taken to be part of the t-tubular network, an assumption supported by their dimensions and proximity to the Z line (fig. 2, right), which are similar to those reported previously (Soeller & Cannell, 1999), although it is not possible to determine whether they are open to the extracellular space. The EM images in figure 2 show that the gross structure of the cell appears to be well maintained following detubulation, although there are fewer apparent t-tubules in the formamide-treated cell; table 1 shows that the main change following formamide treatment is a decrease in the number of t-tubules per unit area, although the area of each t-tubule appears to be unchanged. These changes are compatible with previous data showing that following detubulation, the t-tubules appear to collapse into the cell to form longitudinal vacuoles rather than maintaining their transverse location at the Z-lines (Brette *et al.*, 2002). These data suggest that neither incomplete detubulation, nor distortion of the remaining t-tubules can account for the discrepancy.

Could low specific capacitance of the t-tubule membrane contribute to the discrepancy?

It has previously been reported that in striated muscle the t-tubule membrane is rich in cholesterol, compared with the surface membrane (Rosemblatt *et al.*, 1981;Sumnicht & Sabbadini, 1982). To investigate whether this could reduce the capacitance of the t-tubule membrane sufficiently to account for the discrepancy, we determined the effect of increasing the cholesterol content of a DOPC monolayer, as described in Methods. In the absence of cholesterol, this membrane has a specific capacitance of 1.8 μF/cm^2, twice that (0.9 μF/cm^2) of a bilayer, which in turn is similar to that of the normal cell membrane (1 μF/cm^2). Figure 3 shows that increasing the mole fraction of cholesterol in the DOPC monolayer results in a decrease in its specific capacitance, to ~1 μF/cm^2 (0.56 of control); at 0.3-0.4 mole fraction cholesterol. Increasing cholesterol content above 0.4 mole fraction caused no further decrease in specific capacitance; indeed a small increase occurred, concurrent with phase separation (Whitehouse *et al.*, 2004). Thus it appears that high cholesterol in the t-tubule membrane could decrease its specific capacitance, resulting in a smaller fractional loss of capacitance than of tubular membrane following detubulation.

Can incomplete detubulation plus low specific capacitance account for the discrepancy?

The data presented above suggest that a combination of incomplete detubulation (7.7% of t-tubules remaining) and reduced specific capacitance of the tubular membrane (due, for example, to high cholesterol) might account for the discrepancy between electrophysiological and optical estimates of the percentage of membrane in the t-tubules. To explore this suggestion quantitatively, we used a previously described biophysically realistic computer model of the rat cardiac myocyte (Pasek *et al.*, 2006) that incorporates a t-tubular compartment constituting 56% of the cell membrane. Using this model we determined the loss of membrane capacitance that would be observed upon detubulation if 7.7% of the t-tubules remained functionally coupled to the surface membrane, and the specific capacitance of the t-tubule membrane was 0.56 that of the surface membrane (i.e. the maximal fractional decrease observed on increasing cholesterol content, and assuming the cholesterol content of the surface membrane to be 0%). Figure 4 (top) shows the percentage loss of capacitance that would occur with different percentage losses of tubular membrane in the model; each black line represents a different t-tubule membrane specific capacitance: reducing t-tubule specific capacitance to 0.56 that of the surface membrane and leaving 7.7% of the t-tubule network intact (i.e. ~92% loss of tubular membrane) results in a greater loss of membrane capacitance (~38%) than that observed experimentally (32%). However if the percentage of the cell membrane in the t-tubules is reduced to 49 %, then 32% of membrane capacitance is lost

following detubulation (red line). This assumes the maximum measured decrease in specific capacitance of the t-tubule membrane; if the specific capacitance is higher, then the percentage of the cell membrane in the t-tubules would have to be lower to reconcile the capacitance and optical measurements; the lower panel of figure 4 shows the combinations of specific capacitance and percentage of membrane in the t-tubule that satisfy 32% loss of capacitance. This suggests therefore that 49% may be an upper limit, and thus that optical measurements overestimate the percentage of the cell membrane in the t-tubules while the capacitance measurements underestimate it, although it remains possible that other factors contribute to the discrepancy: for example if factors other than cholesterol reduce the specific capacitance of the t-tubule membrane. However it appears likely that the actual value lies between 49% and 35%, the value obtained from capacitance measurements corrected for incomplete detubulation only; i.e. assuming that the specific capacitance of the t-tubule membrane is the same as that of the surface membrane.

Effect of altered estimates of t-tubular membrane on calculated distribution of ion flux pathways
Incomplete detubulation, or loss of a greater area of membrane than suggested by capacitance measurements, will alter the calculated distribution of ion flux pathways between the t-tubule and surface membranes: incomplete detubulation will result in an underestimate of the fraction of ion flux pathways within the t-tubules, while loss of a greater fraction of membrane than suggested by capacitance measurements will result in a decrease in the calculated density of ion flux pathways in the t-tubules.

We therefore used values that reconcile the optical and electrophysiological measurements of t-tubule area (t-tubule specific capacitance 0.56 μF/cm^2, 49% of the cell membrane within the t-tubules, 7.7% remaining after detubulation, assuming that this is also the fraction electrically coupled to the surface membrane) in the rat ventricular myocyte model described above, to determine the percentage of key membrane currents that would need to be present in the t-tubules to give previously published values determined using detubulation.

Table 2 shows the results of these calculations. The left column shows previously published percentage losses of current following detubulation (and therefore by implication in the t-tubules) corrected, where necessary, for the presence of the 13% of myocytes that show no detubulation (Kawai *et al.*, 1999); it is worth noting that only 13% of I_{Ca} remains after detubulation, putting an upper limit of 13% on the fraction of the t-tubule network remaining, assuming homogeneous current distribution within the t-tubules). The second column shows these values corrected for the presence of 7.7% of the t-tubule network after detubulation. The third

column shows the fraction of each ion flux pathway that has to be located within the t-tubules in the model to give the fraction of current determined experimentally by detubulation; these calculations assume that the current measured experimentally is uncontaminated by other currents flowing under the experimental conditions used. These values differ from those in column two because of factors such as ion concentration changes in the restricted diffusion space of the t-tubules. The fourth column shows a similar calculation for the fraction of ion flux pathways, but after correction for possible contamination by other currents flowing under the experimental conditions used. Table 3 shows the parameters underlying the densities of ion flux pathways at the t-tubule and surface membranes in the model, calculated from the data in table 2 with the t-tubular fraction of the cell membrane set to 49%. This shows the effect of correcting for current fraction on current density, in particular that computation of current densities from loss of currents following detubulation results in underestimation of densities at the t-tubule membrane and overestimation at the surface membrane. An initial description of the effects of these corrections on the behaviour of the rat ventricular myocyte model is given in the companion paper by Pasek *et al.* (2007).

Discussion

Consequences of incomplete detubulation and reduced specific capacitance of tubular membrane

Incomplete detubulation will result in a small underestimate of the fraction of the cell membrane, and of the absolute amount of each membrane current, within the t-tubules (table 2). However it will have a negligible effect on the calculated density of the current within the t-tubules or on the relative amount of each current, assuming that the currents are homogeneously distributed throughout the t-tubule so that the remaining t-tubule membrane has a similar current composition to that lost during detubulation.

If the specific capacitance of the t-tubule membrane is lower than that of the surface membrane, then a given percentage loss of capacitance represents a greater percentage loss of cell membrane. Thus estimating the t-tubular fraction of the cell membrane from loss of capacitance following detubulation will result in an underestimate. This will have no effect on the absolute or relative current loss following detubulation. However correction for this effect will reduce calculated current density. If the fraction of current calculated to be in the t-tubules (table 2) is similar to the corrected fraction of t-tubule membrane (49%), then the t-tubules may not represent a specialized site in terms of density of these proteins. Nevertheless some currents, including I_{Ca} and $I_{Na/Ca}$, are clearly localized at the t-tubules to an extent that is difficult to explain in terms other than t-tubular concentration of protein function: >90% of I_{Ca} for example appears to be in the t-tubules; this fraction is far higher than the upper estimates of the fraction of cell membrane within the t-tubules. It has been reported that some currents are modulated differently at the t-tubule and surface membranes. I_{Ca} for example, appears to be more tightly regulated by PKA and Ca at the t-tubules than at the surface membrane (Brette *et al.*, 2004a). Thus the concentration of protein function at the t-tubules may be due to concentration of the protein, as suggested by immunohistochemical studies, and/or local upregulation of protein function.

These data suggest that the t-tubules show specialisation in either the density and/or regulation of some membrane currents. This has important implications for the trafficking and targeting of membrane proteins; a higher density and better regulation of proteins such as the L-type Ca channel suggest that this protein is trafficked and/or targeted specifically to the t-tubule membrane where it is able to co-localise with regulatory proteins and RyR. Although the mechanisms underlying the trafficking of the cardiac Ca channel to the cell membrane are starting to be elucidated, the mechanisms by which it is targeted to the t-tubule and co-localised with RyR at an apparently stable stoichiometry (Brette *et al.*, 2006b) are unknown. However it has recently

12

been shown that the $\alpha_2\delta$ subunit of $Ca_V2.1$ is completely concentrated in cholesterol rich microdomains in the cerebellum, where it co-localises with the α_1, pore forming, subunit (Davies *et al.*, 2006). A similar mechanism might account for concentration of Cav1.2 in cholesterol rich t-tubule membrane: if, as suggested below, cholesterol is found predominantly in the transverse elements of the t-tubule system, this would be consistent with immunohistochemical data showing localization of the Ca channel to the transverse elements (Brette *et al.*, 2006a).

Conversely, a similar density in the t-tubule and surface membranes suggests that the protein is trafficked/targeted to all parts of the cell membrane and not especially to the t-tubules. However since membrane composition can alter protein function it is also possible that a high cholesterol concentration in the t-tubule membrane may itself alter the function of proteins located in the t-tubule membrane, although a recent study has shown that the cholesterol-depleting agent methyl-β-cyclodextrin has no significant effect on I_{Ca} in rat ventricular myocytes (Calaghan & White, 2006).

Structural changes associated with detubulation

The extent of detubulation was estimated from confocal images of rat ventricular myocytes stained by extracellular application of the lipophilic dye di-8-ANEPPS, using "thresholding" as described previously to exclude background and noise from the analysis. This assumes that the whole t-tubule network is stained using di-8-ANEPPS; it is striking, however, that cells stained in this way show marked transverse striations, but little of the longitudinal elements that have been demonstrated using other techniques; the present data suggest, for example, that ~15% of the cell interior shows t-tubular staining using di-8-ANEPPS, whereas the data of Soeller and Cannell (1999) suggest that the figure should be closer to 30%, if all elements of the t-tubular network shown using their optical method were present. Since di-8-ANEPPS is lipophilic, one possibility is that the lipid (e.g. cholesterol) content of the t-tubule network is higher in the transverse elements. Even in this case it seems likely that the percentage loss of stained elements of the t-tubules system reflects the percentage loss of the whole network. However if cholesterol decreases specific capacitance but is inhomogenously distributed in the t-tubule network, this will further complicate estimation of the percentage of the cell membrane located within the t-tubules from capacitance measurements.

We also used TEM to investigate cell structure following detubulation; this showed that the cell structure was generally well maintained, although there were fewer t-tubules per unit area of cell. This is compatible with previous work suggesting that during detubulation the t-tubules are

detached from, and therefore no longer "held up" by, the surface membrane. As a result they collapse down into their longitudinal elements to form longitudinal vacuoles within the cell (Brette *et al.*, 2002). These changes would also be expected to disrupt dyads within the center of the cell, as suggested previously to account for the lack of sparks in the center of detubulated myocytes (Brette *et al.*, 2005).

Effect of cholesterol on membrane capacitance

Previous work suggests that the skeletal t-tubule membrane is rich in cholesterol (Rosemblatt *et al.*, 1981; Sumnicht & Sabbadini, 1982); however the composition of the cardiac t-tubule membrane is unknown, although caveolae, specialized areas of the cell membrane rich in cholesterol and sphingolipids, are found in the t-tubules. The contribution of caveolae is normally neglected in geometric estimations of surface area, although they account for 14-21% of the surface and t-tubule membranes (Page, 1978), whereas they are taken into account in capacitance measurements. These "little caves", by forming indentations in the t-tubule membrane, may increase its surface area; thus the >50% of the cell membrane within the t-tubules obtained from the optical data of Soeller and Cannell (1999) by approximating the t-tubules to cylinders may be an underestimate. In the present study we modeled the t-tubules using a specific capacitance 0.56 that of the surface membrane, since this was the maximum reduction of specific capacitance obtained by addition of cholesterol to an artificial membrane. This therefore assumes ~40% cholesterol in the t-tubule membrane and 0% in the surface membrane, although such extreme differences are unlikely. In skeletal muscle it has been reported that the cholesterol fraction of the surface membrane ranges from 0.28 to 0.38 (Rosemblatt *et al.*, 1981;Sumnicht & Sabbadini, 1982), and that of the t-tubule membrane is double that of the surface membrane, i.e. 0.56 to 0.76; extrapolating from figure 3 these data suggest that at least in skeletal muscle the specific capacitance of the t-tubule membrane may actually be higher than that of the surface membrane. However the equivalent values for cardiac muscle are unknown, and the different responses to methyl-β-cyclodextrin in the 2 muscle types (below) suggest that they may be different.

Since the cholesterol content of the t-tubule and surface membranes is unlikely to be 40 and 0% respectively, it is likely that the t-tubular fraction of the cell membrane calculated using these values (49%; see above) is an upper limit. This suggests that the optical method of Soeller and Cannell (1999) may overestimate the t-tubular fraction. The reason for this is unclear, but there are two critical factors in the calculation: (i) t-tubule area/cell volume (0.44 $\mu m^2/\mu m^3$); this (and hence t-tubular fraction) could be overestimated in two ways. First, if the dimensions of a

typical t-tubule were overestimated by 100 nm in each axis (the maximum for the sampling parameters used), this would increase the apparent t-tubule area/cell volume ratio; however it is unlikely that such an error would be systematic and it would in any case be compensated by an increase in total surface area/volume, so the t-tubule fraction would remain almost unchanged. Secondly, dye accumulation and the non-ratiometric method used to image fluorescence may lead to overestimation, although the authors provide evidence that such accumulation is unlikely to have been a problem. (ii) total surface area/volume ratio; underestimating this ratio will result in an overestimate of fractional t-tubule area. The total surface area is calculated from measured membrane capacitance, assuming a specific capacitance of 1 $\mu F/cm^2$. However if this assumed value is too high, cell surface area will be underestimated and the fraction of the membrane in the t-tubules will be overestimated: if the specific capacitance of the t-tubule membrane is assumed to be 0.56 $\mu F/cm^2$ and the fraction of cell membrane in the t-tubules to be 0.56, then 38% of capacitance will be lost following detubulation (assuming that 8% of the t-tubule network remains attached; fig. 4 above). If the same values are used to convert the capacitance/volume ratios determined by Satoh *et al.* (1996) to surface area/volume ratios (0.897 - 1.179 cm^2/cm^3), these can be used to calculate the t-tubule membrane fraction from the data of Soeller and Cannell (1999; see Introduction) as between 49% and 37%, assuming accurate measurement of cell capacitance, uncontaminated by membrane currents and accurately calculated from the experimental records: it is possible that membrane capacitance is underestimated by integration of the capacitance current (Christe *et al.*, 2006). However, a similar relative error is made when measuring the capacitance of intact and detubulated cells, so that their ratio is not significantly altered (Christe *et al.*, 2006). Calculation of cell volume is also not straightforward. Soeller and Cannell (1999) assumed a cylindrical cell 100 µm long x 20 µm diameter to calculate total surface area/volume ratio, and hence a t-tubular membrane fraction of 65% (see Introduction). However an elliptical cross-section provides a volume estimate closest to 3D rendered volume (Satoh *et al.*, 1996), and increases the surface area/volume ratio so that the estimated t-tubular membrane fraction decreases by ~10%. This may still be an upper limit because for an ellipsoid cell the rendered volume is 29% smaller than the computed volume, so that the surface area/volume ratio may be even larger (Satoh *et al.*, 1996). Although capacitance/volume ratios obtained in adolescent Sprague Dawley rats (6.76 pF/pl; Satoh et al., 1996) provide values that agree with the surface area/volume ratio calculated by Soeller and Cannell (1999; see Introduction), this may not be an appropriate reference for measurements in Wistar rats: a recent study reports an average ventricular myocyte volume and capacitance of 23.6 pl and 200 pF respectively in 300g adult Wistar rats (Swift *et al.*,

15

2006), giving a total membrane capacitance/volume ratio of 8.43 pF/pl, close to that of 8.88 pF/pl obtained in adult Sprague Dawley rats (Satoh et al. 1996). Combined with the t-tubule area/volume ratio of Soeller and Cannell (1999), this provides a t-tubule fraction of 52%. Interestingly, detubulation of ventricular cells from Sprague Dawley rats results in similar losses of cell capacitance (32%; Despa et al. 2003) as in the Wistar rats used in the present study.

Previous work investigating the effect of cholesterol on membrane capacitance has shown either a decrease, no change, or increase in membrane capacitance. Interestingly a recent study using the cholesterol-depleting agent methyl-β-cyclodextrin showed no change in membrane capacitance or t-tubule structure in rat ventricular myocytes (Calaghan & White, 2006), although previous work has shown that methyl-β-cyclodextrin disrupts the t-tubules in myotubes (Pouvreau *et al.*, 2004), so that the structure of skeletal and cardiac t-tubules may rely to different extents on cholesterol. It might be expected, however, that insertion of cholesterol in the membrane would increase membrane thickness, and thus decrease capacitance. In the present study we used an artificial monolayer, and showed that cholesterol reduced membrane capacitance. Although a useful experimental system with a capacitance similar to that of the cell membrane, this membrane differs from that in the cell: for example it is a monolayer rather than a bilayer, its composition is simpler than that of the cell membrane, it is not in contact with proteins, and it is exposed to different mechanical stresses.

Nevertheless the present work suggests that the specific capacitance of the t-tubule membrane may be lower than that of the surface membrane, possibly because of a high cholesterol content; correction for such an effect would increase the fraction estimated by detubulation and decrease the fraction calculated from optical measurements, and could therefore help reconcile the estimates of t-tubule membrane fraction obtained using the two methods; the considerations discussed above suggest that the true fraction lies close to 50%: between the values obtained using the two techniques.

Acknowledgements

Reference

Bers DM (2001). *Excitation-contraction coupling and cardiac contractile force* 2nd ed. Dordrecht, Netherlands: Kluwer Academic.

Bers DM (2002). Cardiac excitation-contraction coupling. *Nature* **415**, 198-205.

Bizzotto D & Nelson A (1998). Continuing electrochemical studies of phospholipid monolayers of dioleoyl phosphatidylcholine at the mercury-electrolyte interface. *Langmuir* **14**, 6269-6273.

Brette F, Despa S, Bers DM, & Orchard CH (2005). Spatiotemporal characteristics of SR Ca^{2+} uptake and release in detubulated rat ventricular myocytes. *J Mol Cell Cardiol* **39**, 804-812.

Brette F, Komukai K, & Orchard CH (2002). Validation of formamide as a detubulation agent in isolated rat cardiac cells. *Am J Physiol* **283**, H1720-H1728.

Brette F, Leroy J, Le Guennec JY, & Salle L (2006a). Ca^{2+} currents in cardiac myocytes: Old story, new insights. *Prog Biophys Mol Biol* **91**, 1-82.

Brette F & Orchard C (2003). t-tubule function in mammalian cardiac myocytes. *Circ Res* **92**, 1182-1192.

Brette F & Orchard CH (2006a). Density and sub-cellular distribution of cardiac and neuronal sodium channel isoforms in rat ventricular myocytes. *Biochem Biophys Res Commun* **348**, 1163-1166.

Brette F & Orchard CH (2006b). No apparent requirement for neuronal sodium channels in excitation-contraction coupling in rat ventricular myocytes. *Circ Res* **98**, 667-674.

Brette F, Rodriguez P, Komukai K, Colyer J, & Orchard CH (2004a). beta-adrenergic stimulation restores the Ca transient of ventricular myocytes lacking t-tubules. *J Mol Cell Cardiol* **36**, 265-275.

Brette F, Salle L, & Orchard CH (2004b). Differential modulation of L-type Ca^{2+} current by SR Ca^{2+} release at the t-tubules and surface membrane of rat ventricular myocytes. *Circ Res* **95**, e1-e7.

Brette F, Salle L, & Orchard CH (2006b). Quantification of calcium entry at the t-tubules and surface membrane in rat ventricular myocytes. *Biophys J* **90**, 381-389.

Calaghan S & White E (2006). Caveolae modulate excitation-contraction coupling and beta2-adrenergic signalling in adult rat ventricular myocytes. *Cardiovasc Res* **69**, 816-824.

Christe G, Zhang Y, Ricci E, Chouabe C, & Bonvallet R (2006). Evaluation of cardiac cell membrane capacitance from the current response to a small pulse. Compared reliability of numerical integration versus fitting an exponential decay. *Proc Physiol Soc 3* **PC99**, (Abstract).

Cohen-Atiya M, Nelson A, & Mandler D (2006). Characterization of n-alkanethiol self-assembled monolayers on mercury by impedance spectroscopy and potentiometric measurements. *Journal of Electroanalytical Chemistry* **593**, 227-240.

Davies A, Douglas L, Hendrich J, Wratten J, Tran Van MA, Foucault I, Koch D, Pratt WS, Saibil HR, & Dolphin AC (2006). The calcium channel alpha$_2$delta-2 subunit partitions with Ca$_V$2.1 into lipid rafts in cerebellum: implications for localization and function. *J Neurosci* **26**, 8748-8757.

Despa S, Brette F, Orchard CH, & Bers DM (2003). Na/Ca exchange and Na/K-ATPase function are equally concentrated in transverse tubules of rat ventricular myocytes. *Biophys J* **85**, 3388-3396.

Heinzel FR, Bito V, Volders PG, Antoons G, Mubagwa K, & Sipido KR (2002). Spatial and temporal inhomogeneities during Ca^{2+} release from the sarcoplasmic reticulum in pig ventricular myocytes. *Circ Res* **91**, 1023-1030.

Kawai M, Hussain M, & Orchard CH (1999). Excitation-contraction coupling in rat ventricular myocytes after formamide-induced detubulation. *Am J Physiol* **277**, H603-H609.

Komukai K, Brette F, Yamanushi TT, & Orchard CH (2002). K$^+$ current distribution in rat sub-epicardial ventricular myocytes. *Pflugers Arch* **444**, 532-538.

Nelson A & Auffret N (1988). Phospholipid monolayers of di-oleoyl lecithin at the mercury/water interface. *Journal of Electroanalytical Chemistry* **244**, 99-113.

Page E (1978). Quantitative ultrastructural analysis in cardiac membrane physiology. *Am J Physiol* **235**, C147-C158.

Pandit SV, Clark RB, Giles WR, & Demir SS (2001). A mathematical model of action potential heterogeneity in adult rat left ventricular myocytes. *Biophys J* **81**, 3029-3051.

Pásek M, Šimurda J, & Christé G (2006). The functional role of cardiac t-tubules explored in a model of rat ventricular myocytes. *Philos Transact A Math Phys Eng Sci* **364**, 1187-1206.

Pásek M, Šimurda J, Christé G, & Orchard CH (2007). Modelling the cardiac transverse-axial tubular system. *Prog Biophys Mol Biol* (this issue).

Pouvreau S, Berthier C, Blaineau S, Amsellem J, Coronado R, & Strube C (2004). Membrane cholesterol modulates dihydropyridine receptor function in mice fetal skeletal muscle cells. *J Physiol* **555**, 365-381.

Rosemblatt M, Hidalgo C, Vergara C, & Ikemoto N (1981). Immunological and biochemical properties of transverse tubule membranes isolated from rabbit skeletal muscle. *J Biol Chem* **256**, 8140-8148.

Satoh H, Delbridge LM, Blatter LA, & Bers DM (1996). Surface:volume relationship in cardiac myocytes studied with confocal microscopy and membrane capacitance measurements: species-dependence and developmental effects. *Biophys J* **70**, 1494-1504.

Soeller C & Cannell MB (1999). Examination of the transverse tubular system in living cardiac rat myocytes by 2-photon microscopy and digital image-processing techniques. *Circ Res* **84**, 266-275.

Sumnicht GE & Sabbadini RA (1982). Lipid composition of transverse tubular membranes from normal and dystrophic skeletal muscle. *Arch Biochem Biophys* **215**, 628-637.

Swift F, Stromme TA, Amundsen B, Sejersted OM, & Sjaastad I (2006). Slow diffusion of K^+ in the T tubules of rat cardiomyocytes. *J Appl Physiol* **101**, 1170-1176.

Voigt T & Dauber W (2004). About the T-system in the myofibril-free sarcoplasm of the frog muscle fibre. *Tissue and Cell* **36**, 245-248.

Whitehouse C, O'Flanagan R, Lindholm-Sethson B, Movaghar B, & Nelson A (2004). Application of electrochemical impedance spectroscopy to the study of dioleoyl phosphatidylcholine monolayers on mercury. *Langmuir* **20**, 136-144.

Wier WG & Balke CW (1999). Ca^{2+} release mechanisms, Ca^{2+} sparks, and local control of excitation-contraction coupling in normal heart muscle. *Circ Res* **85**, 770-776.

Yang Z, Pascarel C, Steele DS, Komukai K, Brette F, & Orchard CH (2002). Na^+-Ca^{2+} exchange activity is localized in the t-tubules of rat ventricular myocytes. *Circ Res* **91**, 315-322.

	(a) Area of myocyte analysed (μm^2)	(b) Area within (a) occupied by t-tubules (μm^2)	(b/a)*100 (%)	Number of t-tubules	t-tubules/μm^2	Average t-tubule area (μm^2)
Control	131.40 ± 8.98	2.66 ± 0.63	1.93 ± 0.38	55 ± 9	0.37 ± 0.03	0.046 ± 0.006
Detubulated	127.20 ± 5.82	1.16 ± 0.23*	0.94 ± 0.20*	28 ± 5*	0.22 ± 0.04*	0.046 ± 0.009

Table 1. T-tubule characteristics determined from TEM images of control and detubulated rat ventricular myocytes, obtained as described in Methods. * P<0.05 compared with control myocytes. n = 431 t-tubules in 8 control cells; 166 t-tubules in 6 detubulated cells.

	Experimental data		Fraction from model	
	Loss of current	Corrected for incomplete detubulation	From uncontaminated current	After accounting for contamination by other currents
I_{Na} (1)	32 %	35 %	38 %	38 %
I_{Ca} (2)	87 %	94 %	96 %	95 %
I_{Kto} (3)	32 %	40 %	41 %	46 %
I_{Kss} (3)	76 %	82 %	85 %	86 %
I_{K} (3)	32 %	40 %	-	-
I_{K1} (3)	32 %	40 %	47 %	47 %
I_{NaCa} (4)	63 %	68 %	72 %	78 %
I_{NaK} (4)	59 %	64 %	64 %	64 %

Table 2. Use of a biophysically realistic computer model of a rat ventricular myocyte (specific capacitance of the t-tubule membrane 0.56 µF/cm^2, 49% of the cell membrane within the t-tubules, 7.7% of the t-tubule network remaining after detubulation, and assuming that this fraction is electrically coupled to the surface membrane) to calculate the percentage of each ion flux pathway necessary within the t-tubules (right columns) to give the percentages of membrane current calculated to be within the t-tubules from experimental data obtained by detubulation (left columns). The bracketed numbers by each membrane current refer to the reference from which the experimental data were obtained, as follows: (1) Brette and Orchard, 2006; (2) Kawai *et al.,* 1999; (3) Komukai *et al.,* 2002; (4) Despa *et al.,* 2003. See text for further information.

	Model before correction			Model after correction		
	t-density	**S-density**	**ratio**	**t-density**	**S-density**	**ratio**
I_{Na}	6.53 mS/cm^2	13.33 mS/cm^2	0.49	7.76 mS/cm^2	12.16 mS/cm^2	0.64
I_{Ca}	3.73e-4 cm/s	5.35e-5 cm/s	6.97	4.07e-4 cm/s	2.06e-5 cm/s	19.77
I_{Kto}	0.229 mS/cm^2	0.467 mS/cm^2	0.49	0.329 mS/cm^2	0.371 mS/cm^2	0.89
I_{Kss}	0.1086 mS/cm^2	0.0329 mS/cm^2	3.30	0.1229 mS/cm^2	0.0192 mS/cm^2	6.39
I_{K1}	0.157 mS/cm^2	0.320 mS/cm^2	0.49	0.230 mS/cm^2	0.249 mS/cm^2	0.92
I_{NaCa}	2.31e-4 μA/cm^2	1.31e-4 μA/cm^2	1.76	2.87e-4 μA/cm^2	7.76e-5 μA/cm^2	3.70
I_{NaK}	1.204 μA/cm^2	0.804 μA/cm^2	1.50	1.306 μA/cm^2	0.706 μA/cm^2	1.85

Table 3. Parameters determining the density of ion flux pathways in the t-tubular (t-density) and surface (S-density) membranes in the model, showing the effect of correcting for current fraction on current density. The densities before correction are calculated from the fractions of tubular ion currents obtained by detubulation ("loss of current" in table 2); those after correction were obtained after incorporating incomplete detubulation, the effect of ion concentration changes within the t-tubules and the effect of contamination by other currents (right column in table 2). The t-tubular fraction of the cell membrane in the model was set to 49%. mS/cm^2: maximum conductance/unit surface area; μA/cm^2: maximum current/unit surface area; cm/s: permeability/unit surface area.
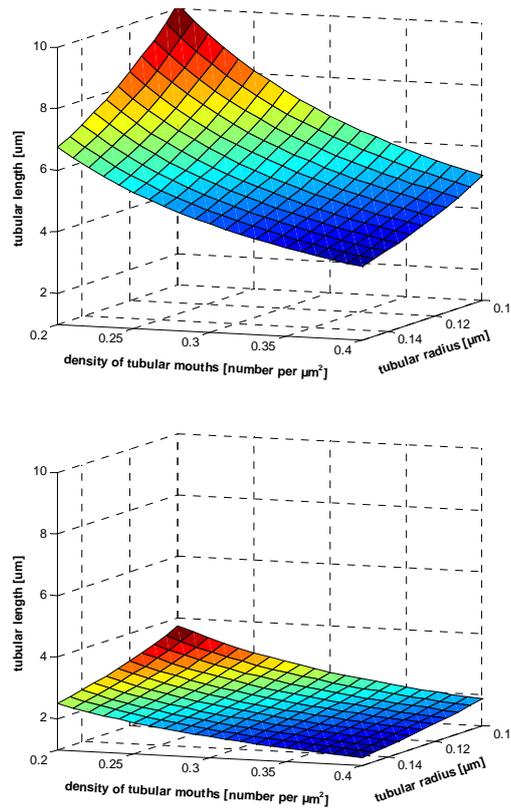
Figure 1. The combinations of density of t-tubule openings, mean tubular radius and mean tubular length that can mathematically coexist in a cardiac myocyte with a t-tubular membrane fraction of either 56% (top) or 32% (bottom). The planes are colour coded to distinguish between long (red) and short (blue) tubular lengths. Comparison of these combinations with published values can help determine which estimate of fractional area of tubular membrane may be closest to the true value; see text for further information.
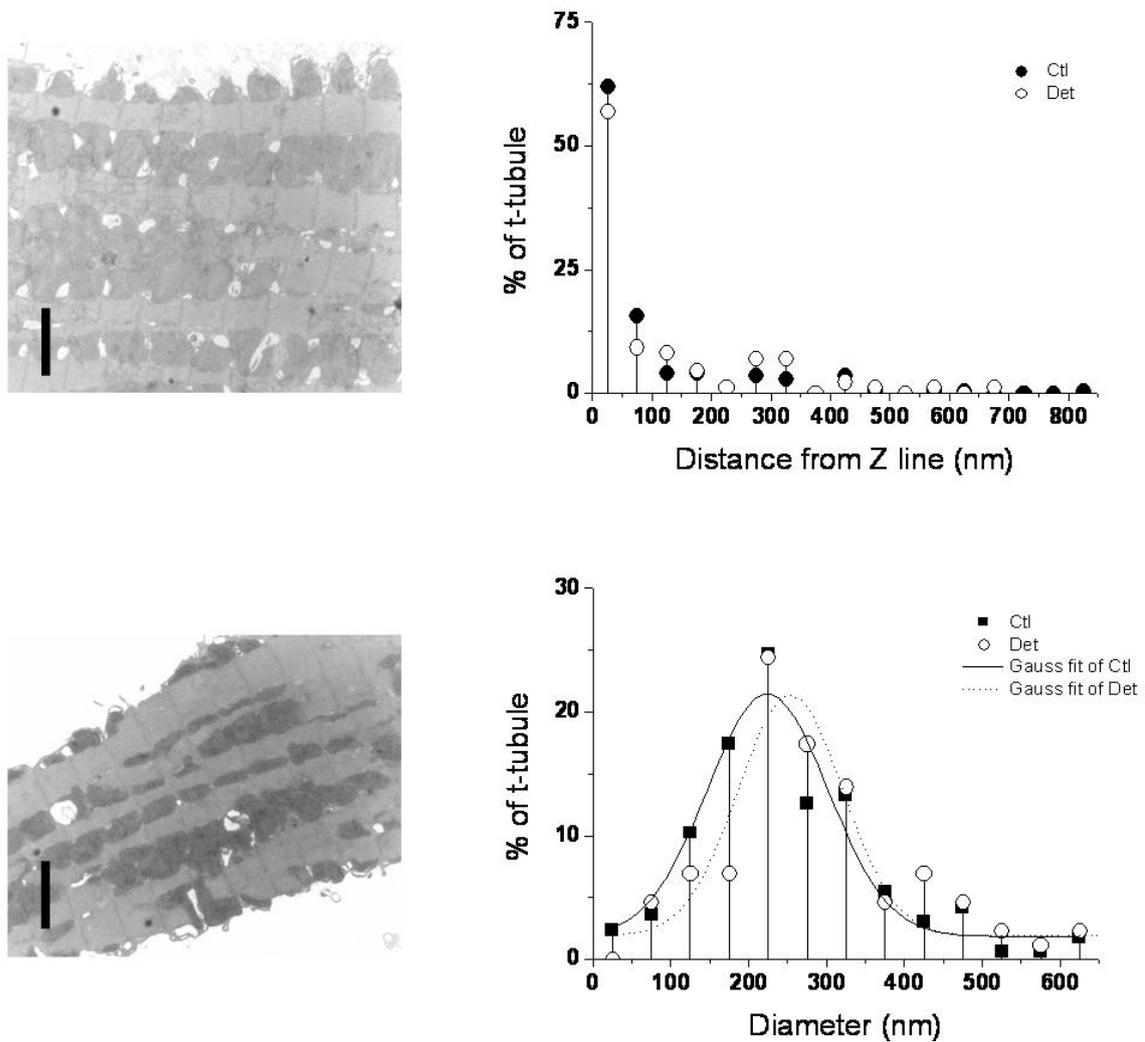
Figure 2. Left: representative transmission EM images of control (top) and detubulated (bottom) rat ventricular myocytes. The bars in each panel represent 2 μm. Right: the distribution of distances of putative t-tubules from the nearest Z-line (top) and the distribution of diameters of putative t-tubules (bottom) in control (filled symbols) and detubulated (open circles) myocytes, with Gaussian fits. n = 166 t-tubules in 4 control cells; 86 t-tubules in 2 detubulated cells.
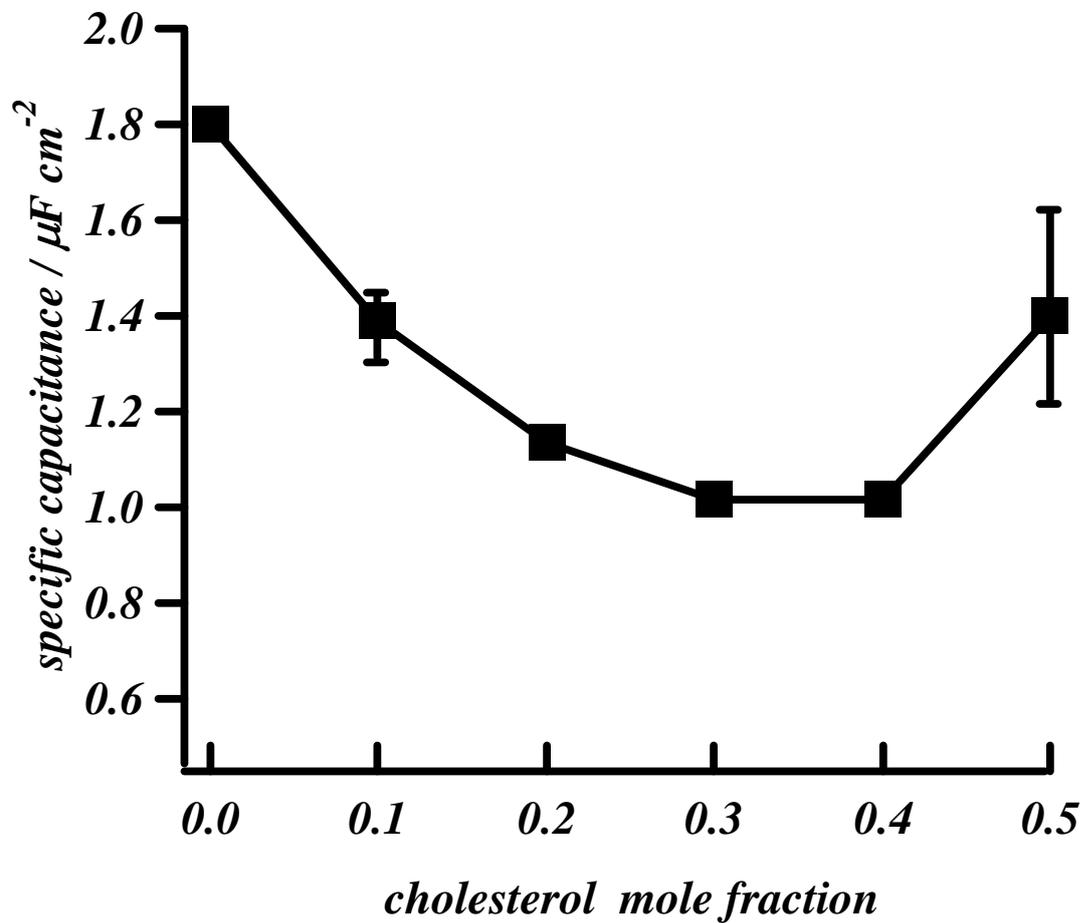
Figure 3.   The effect of cholesterol on specific capacitance, measured as the zero frequency capacitance of a DOPC monolayer-coated mercury electrode with cholesterol incorporation. Experiments carried out in 100 mmol/l KCl.
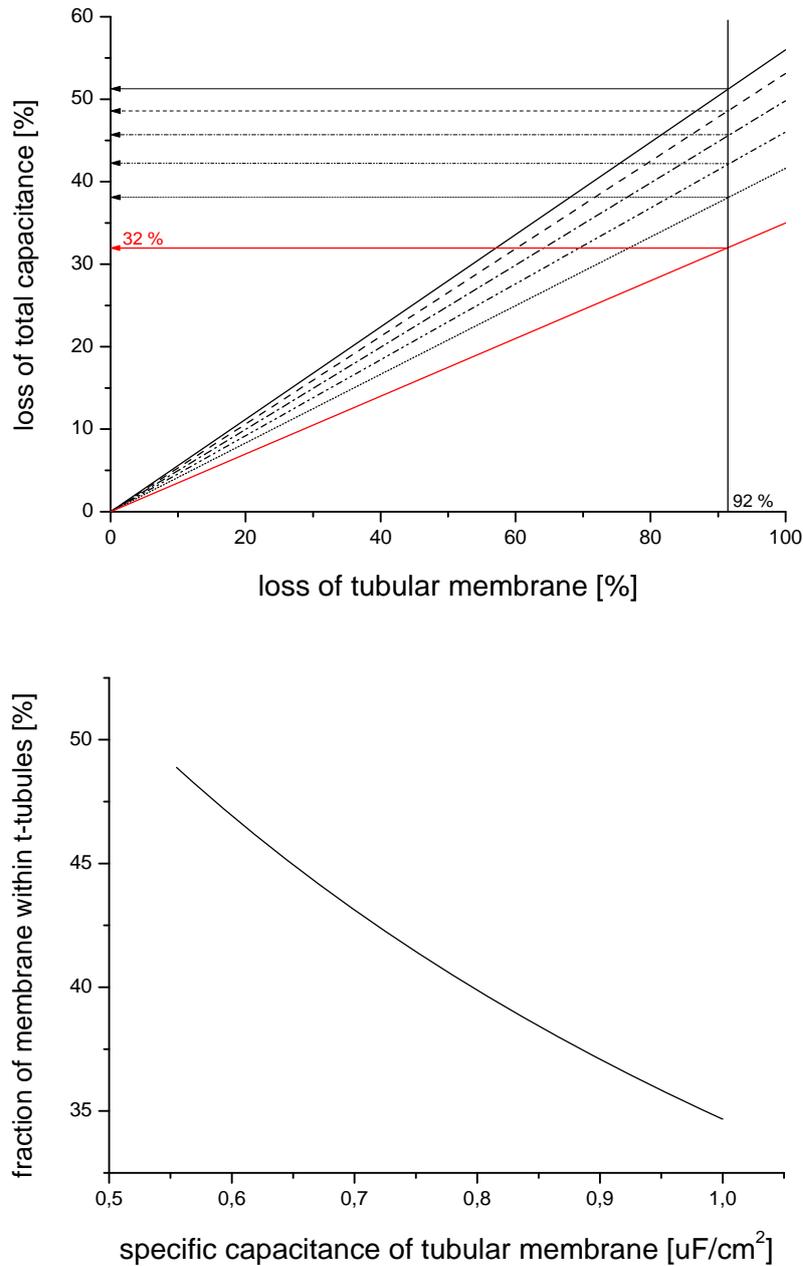
Figure 4. Top: Relation between loss of tubular membrane and loss of total capacitance for different values of specific capacitance of tubular membrane in models with 56 % and 49 % of membrane within t-tubules. The values of specific capacitance in the 56% model are represented by black lines were: 1 [$\mu F/cm^2$] (full line); 0.89 [$\mu F/cm^2$] (dashed line); 0.78 [$\mu F/cm^2$] (dotted line); 0.67 [$\mu F/cm^2$] (dot-dashed line) and 0.56 [$\mu F/cm^2$] (dot-dot-dashed line). The value of specific capacitance in the 49% model (red line) was 0.56 [$\mu F/cm^2$]. 92% represents incomplete detubulation. Bottom: Relation between specific capacitance and percentage of membrane within the t-tubules that satisfies 32% loss of capacitance observed in experiments with incomplete detubulation.